Systems Integration and Test of the Lunar Flashlight Spacecraft

Nathan Cheek
Jet Propulsion Laboratory, California Institute of Technology
4800 Oak Grove Drive, Pasadena, CA 91109; (818) 354-4321
nathan.cheek@jpl.nasa.gov

Collin Gonzalez
The Aerospace Corporation
2310 East El Segundo Boulevard, El Segundo, CA 90245
collin.gonzalez@aero.org

Philippe Adell, John Baker, Chad Ryan, Shannon Statham
Jet Propulsion Laboratory, California Institute of Technology

E. Glenn Lightsey, Celeste R. Smith
Georgia Institute of Technology

Conner Awald, Jud Ready
Georgia Tech Research Institute

ABSTRACT

Lunar Flashlight is a 6U CubeSat launching in late 2022 or early 2023 that will search for surface water ice content in permanently shadowed regions at the south pole of the Moon using infrared relative reflectance spectroscopy. The mission will act as a technology demonstration of an Advanced Spacecraft Energetic Non-Toxic (ASCENT) green propulsion system and active laser spectroscopy within the CubeSat form-factor. This paper provides an overview of the entire Systems Integration and Test campaign which took place at the Jet Propulsion Laboratory and the Georgia Institute of Technology. From initial testing of the isolated avionics and payload subsystems to the final tests with a fully integrated spacecraft, the functional and environmental test campaign is reviewed, with a focus on lessons learned.

PROJECT OVERVIEW

Lunar Flashlight is a 6U CubeSat developed by the NASA Jet Propulsion Laboratory (JPL) in conjunction with the NASA Marshall Space Flight Center (MSFC), the University of California, Los Angeles (UCLA), and the Georgia Institute of Technology (GT). This mission will demonstrate the capabilities of green monopropellant propulsion systems and near-infrared laser spectroscopy within the CubeSat form-factor. The propulsion system, developed by GT and MSFC,[1] will complete a lunar orbit insertion (LOI) and multiple trajectory correction maneuvers (TCMs), placing the 14 kg spacecraft in a near-rectilinear halo orbit about the Moon. Once in lunar orbit, four near-infrared lasers will detect and map, via relative reflectrometry, water ice in permanently-shaded regions near the lunar south pole.[2] This project addresses one of NASA's Strategic Knowledge Gaps: composition, quantity, distribution, form of water/H species, and other volatiles associated with lunar cold traps.[3]

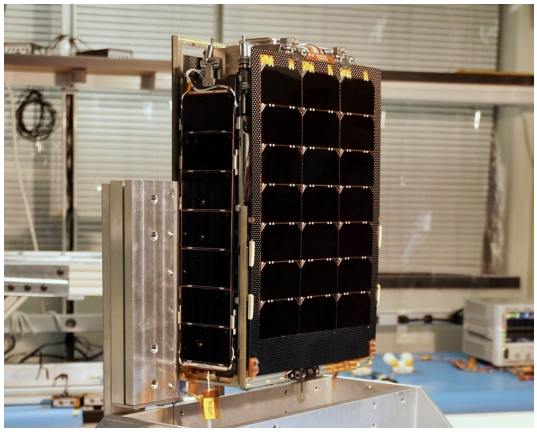

Figure 1: Fully Integrated Spacecraft

Spacecraft Overview

The 6U CubeSat has a mass of approximately 14 kg after fueling, and includes power, command and data handling, communications, attitude control, propulsion, and payload subsystems (Figure 2).

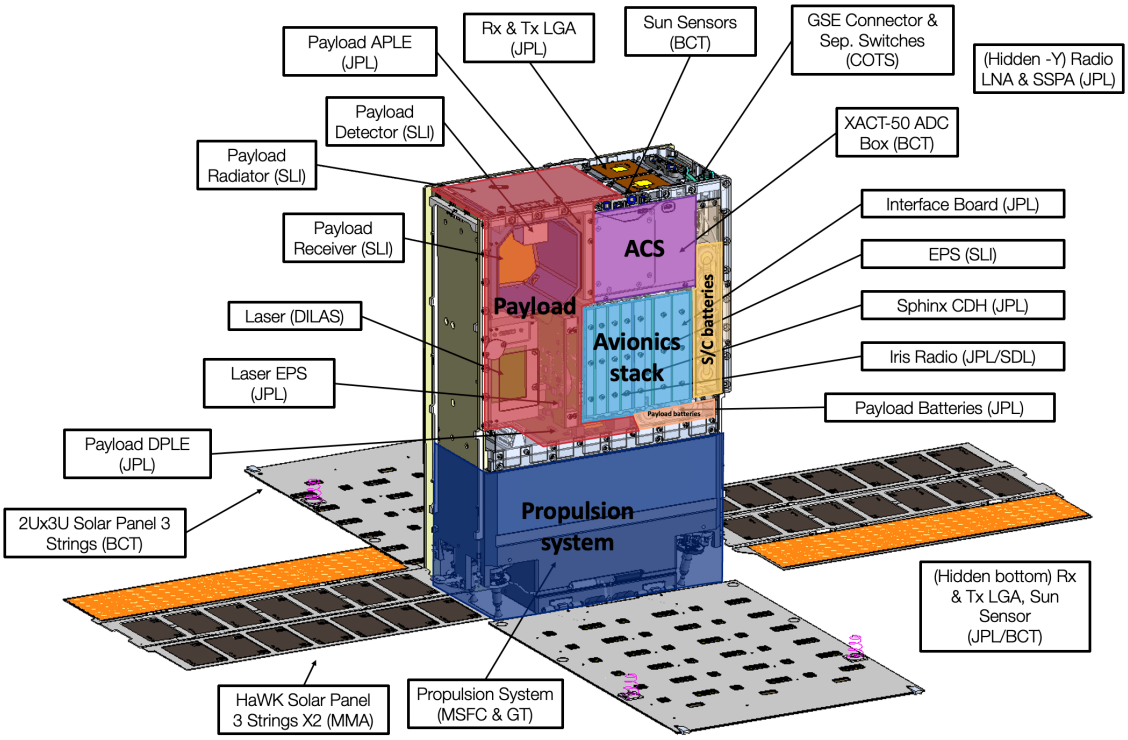

Figure 2: Overview of Spacecraft

The power subsystem includes four solar arrays, developed by Blue Canyon Technologies (BCT) and MMA, along with an Electrical Power Systems (EPS) management board and a battery based on Panasonic NCR18650B cells.[4] The arrays are capable of providing over 55 W at end of life.

Command & Data Handling (C&DH) is provided by a JPL-developed Sphinx single-board computer, which utilizes a GR712RC radiation-hardened microprocessor and a ProASIC3 FPGA. The flight software is built using JPL's F Prime framework.[5]

The spacecraft uses an Iris Radio, developed by JPL and Utah State University's Space Dynamics Laboratory for small satellite telecommunications.[6] A pair of low-gain antennas sits at each end of the spacecraft on the Z-axis, providing transmit and receive capability independent of the spacecraft's orientation.

A BCT XACT-50 acts as the attitude determination and control system (ADCS) for the spacecraft. It utilizes sun sensors mounted around the spacecraft as well as an internal star tracker and three internal reaction wheels.[7]

The Lunar Flashlight Propulsion System (LFPS) was designed and built by Georgia Tech's Glenn Lightsey Research Group in collaboration with the NASA Marshall Space Flight Center.[8] It can provide over 3300 N s of impulse, allowing for lunar orbit insertion, correctional maneuvers, and reaction wheel desaturation during the mission.[9]

Lunar Flashlight's science instrument payload is a compact Short Wave Infrared (SWIR) Laser reflectometer designed to find signatures of water ice in the lunar regolith. Diode lasers emit infrared energy at four different wavelengths sequentially. This light reflects off the lunar surface and is picked up by the onboard paraboloidal receiver mirror which collects the incoming light onto an InGaAs detector.[10] Differences in the detector's amplitude across the sequence can be used to identify the water ice signature.[2] Due to high power requirements for the lasers, they are powered from a separate battery based on Sony NCR18650B cells.[4]

SI&T Overview

The goal of the Systems Integration and Test (SI&T) process was to integrate each subsystem into a single cohesive system, build the spacecraft for flight, and confirm its capabilities through an extensive suite of tests. Some subsystems were delivered ready for integration. Other subsystems, such

as the payload, required further development by the SI&T team to meet all functional requirements and interface appropriately with other subsystems.

Mission Assurance

Lunar Flashlight is classified by NASA as a "technology demonstration" payload, governed by NASA 7120.8, and classified by JPL as a "Class D Type II" project. These classifications helped to shape the project's Safety and Mission Assurance Plan (SMAP) as well as the Quality Assurance (QA) Requirements Tailoring Agreement (QARTA).

Various internal tools were utilized at JPL to track the state of hardware during SI&T, including the Instructions/Procedures for Build, Assemble, and Test (IBAT/PBAT) systems, the Quality Assurance Reporting System (QARS), and the Problem Reporting System (PRS). DOORS NG software was used to track requirements.

During final SI&T activities at JPL, QA often acted as a witness to final mates and torques as well as staking of flight hardware. However, the QARTA allowed for peer witness verification of many activities. Additionally, only a few flight hardware items were classified as Quality Critical Items (QCI), which kept oversight requirements limited.

Prior to the delivery of the upper spacecraft to Georgia Tech, JPL mission assurance personnel surveyed GT's facilities for flight SI&T readiness. Once the spacecraft was at GT, JPL Mission Assurance and QA continued to support the project in an oversight role, participating in daily tag-ups, activity planning, and reviews. QA monitored critical activities with a mix of in-person and remote video support.

Integration Practices

Most integration activity at JPL took place in the JPL CubeSat Lab class 300,000 cleanroom, while integration activity at Georgia Tech was primarily done in the C-SHAFT class 100 cleanroom. Preapproved work procedures and a "buddy system" were required for all activity involving flight hardware. Integration work was logged in the IBAT system and captured through extensive photography.

Throughout the SI&T process, the team drew on JPL's in-house Electronic Manufacturing, Packaging & Tech Services section to manage and execute complex board reworks. For other reworks, the project worked directly with JPL technicians, providing Cognizant Engineer (Cog-E) and QA-approved build instructions to the technicians. For mechanical manufacturing and rework activities, the team utilized JPL's Mechanical Fabrication & Test section. Premixed epoxies and other polymerics were provided by JPL's polymerics team.

The team relied on a JPL flight mechanical assembly technician to help build the mechanical assemblies for flight. This technician brought invaluable knowledge, skills, and tooling from their work on larger projects that allowed the team to resolve a number of setbacks.

Once at Georgia Tech, GTRI technicians, students, and engineers performed most integration activities. JPL mechanical engineers were present to support installation of the propulsion system and solar panels, and JPL maintained an on-site SI&T lead as final integration and test activity was performed. Additionally, the JPL mechanical assembly technician flew to Atlanta to support certain in-depth integration tasks.

Test Practices

As with integration procedures, all tests involving flight hardware required pre-approved procedures and use of the "buddy system". Procedures were approved by the deputy project manager, QA, and, when applicable, component Cog-E's. When tests took place in non-cleanroom environments, the team made an effort to keep work surfaces clean and hardware covered as much as possible.

JPL's SI&T team utilized LaTeXto write procedures, which allowed for easy version-control, formatting consistency, and central updating of subprocedures. Multiple test procedures were developed over time into a single "choose your own adventure" full functional test procedure where operators could indicate which components were in a test setup and navigate to the applicable setup or power-on sections. This approach was useful given the evolving nature of the hardware and the limited personnel available to maintain procedures.

Georgia Tech was responsible for authoring and executing most procedures at GT. Joint Test Readiness Reviews (TRRs) were hosted for each activity, allowing for feedback from JPL project management, mission assurance, Cog-E's, and flight engineers. These procedures referenced the JPL SI&T-authored full functional test procedure when completing standard tasks, such as power-on, charging, and software updates.

iPads were used extensively for running procedures at JPL and GT. This approach eliminated paper clutter, added the ability to seamlessly drop in photographs atop placeholder boxes, and made edits and color-coded notes easy to add.

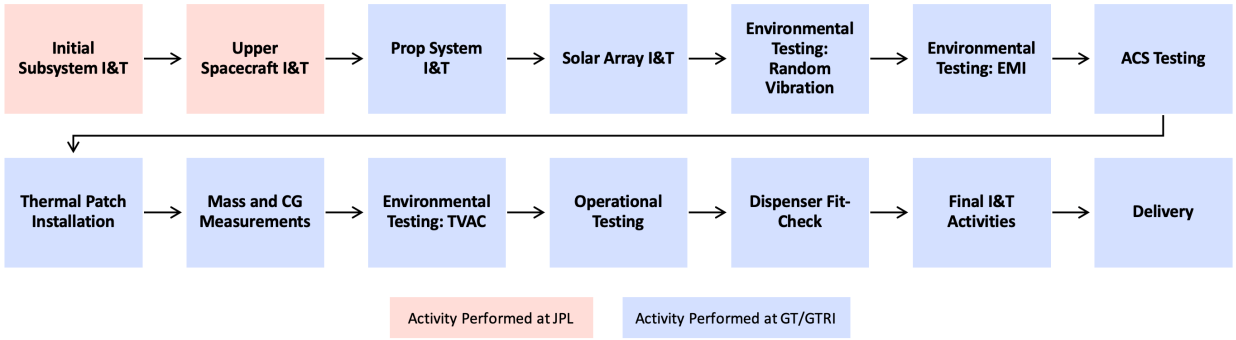

Figure 3: Flow of SI&T Activities

INTEGRATION AND TEST ACTIVITIES

The Lunar Flashlight Systems Integration and Test campaign began at JPL in 2018 with initial work on integrating and testing at the subsystem level. The team followed the flow seen in Figure 3, finishing in 2022 at GT with the delivery of the fully-built and tested spacecraft.

Initial Subsystem I&T

Prior to assembling the spacecraft for flight, an array of integration and test activities were performed with each subsystem. Early in the project, standalone electrical tests took place as components arrived or were reworked. Later on, as the system became more stable and integrated, more complex system-level functional tests were performed.

Initial Avionics Power-On Checkout

Testing of all components began with simple electrical integration, power-on, and telemetry checkout tests. This process began with a "safe-to-mate" of all electrical interfaces. In a typical safe-to-mate, all pins were probed with a digital multimeter (DMM) to measure their unpowered resistance to ground, followed by their powered voltage. The board designer or Cog-E generally provided a list of additional required pin-to-pin measurements, expected values for those measurements when possible, and a warning list of any pins requiring special handling.

Once SI&T was satisfied with the results of the safe-to-mate, the component was integrated into the system. In the primary avionics workflow, SI&T built up the avionics assembly from the C&DH board to the EPS board, radio, and interface board. Figure 4 shows one step of the "avionics stack" buildup as these main components were mated directly via board mounted Tyco 160-pin connectors.

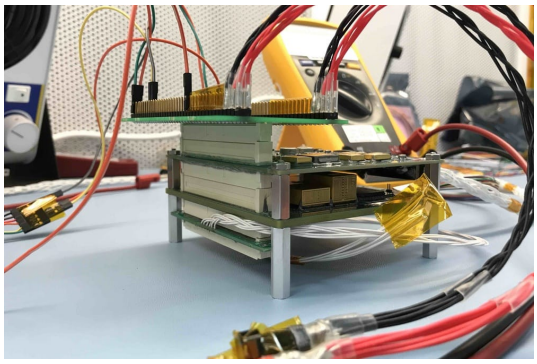

Figure 4: Avionics Stackup Test with EPS and Sphinx

During the initial avionics integration process, the project was able to leverage the commonality of the C&DH, EPS, and Iris radio with the Near-Earth Asteroid Scout (NEA Scout) mission, which also shared some personnel. For example, when NEA Scout found a floating signal between C&DH and EPS boards causing unexpected system resets, Lunar Flashlight was able to implement the hardware fix before beginning testing.

Power-on and setup steps developed in support of this early testing were passed into the full functional test procedure. Additionally, as test data was accumulated, the procedure was updated to inform testers of more accurate expected values and power consumption profiles.

Deep Space Network RF Compatibility Test

The DSN RF compatibility test was conducted at the Peraton DTF-21 facility near Los Angeles and was the only opportunity to test the spacecraft's FSW → C&DH → Iris transceiver → Iris TX/RX amplifier signal chain connected directly to an actual DSN receiver. It also served as an opportunity for the ground data systems team to test their interface to the DSN. As the test occurred prior to much of

the avionics stack being ready for integration, the test was conducted in a flat-sat setup consisting of only the C&DH board and Iris radio system. Testing took place with coaxial wired connections. All flight uplink and downlink configurations were tested, as well as signal lock time and ranging modes.

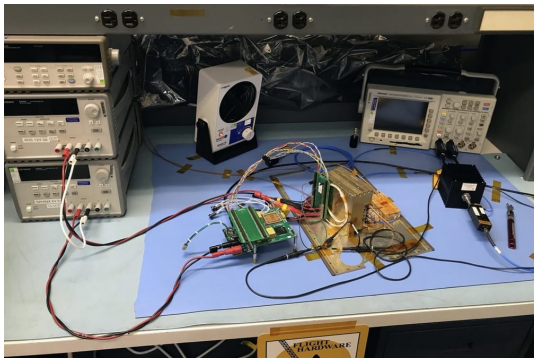

Figure 5: C&DH and Radio Setup for DSN Compatibility Test

Payload End-to-End Tests

As part of the payload's subsystem-level testing, four payload end-to-end (ETE) tests of increasing complexity were conducted. The system configuration evolved from test to test, moving from a "flat-sat" payload configuration in the first test to a fully assembled payload/avionics setup in the final test.

These tests verified a variety of payload performance details, such as power draw characteristics of the lasers and performance of the payload battery. Thermal performance was also tested, verifying the thermal control of the Phase Change Material (PCM) ($18\pm1\,^{\circ}\mathrm{C}$) and radiator ($-61.0\pm0.5\,^{\circ}\mathrm{C}$) with onboard heaters.

Response time and noise performance of the detector's analog front-end measurement chain were iteratively tested and improved.[11] Data was collected to quantify the stability of the laser power drive, laser output power, and laser spectrum with respect to laser temperature over multiple 90-second firings.

The ETE tests also provided an opportunity to control the payload through the flight avionics interface and uncover any operational idiosyncrasies. The payload captures high-speed "experiment data" during laser firing, and the collection, downlinking, and processing of this data was tested extensively.

For these tests, hardware was placed in a thermal vacuum chamber. A two stage cryo-radiator was thermally connected to the receiver housing and radiator using copper sheets, and a recirculating chiller was connected the PCM using a plumbed copper block. GSE heaters were attached to the copper sheets to keep the temperature near the target zone and protect the hardware should the onboard heaters fail.

One challenge the team faced was limiting detector measurement saturation while still firing the 75 W lasers at full power. To accomplish this, a diffuser was placed in the beampath of the laser, and a GSE cover outfitted with a pinhole slot was installed over the receiver window.

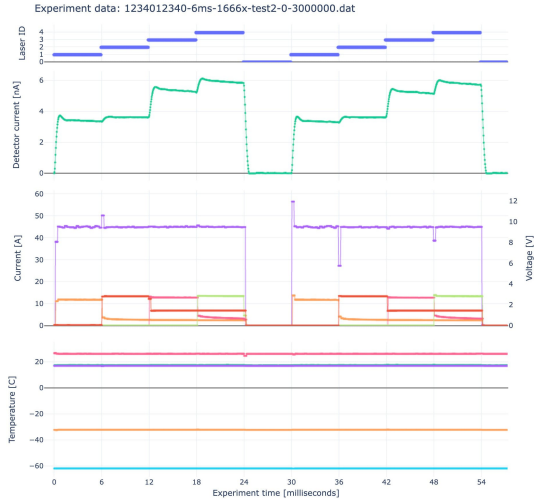

Figure 6: Example ETE Experiment Data

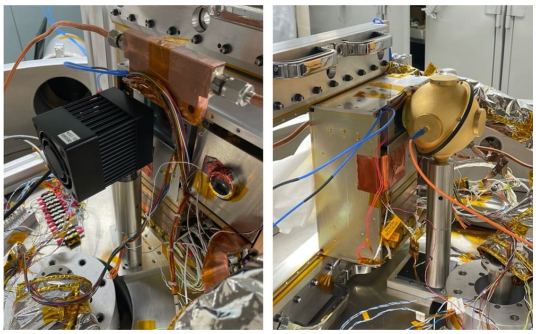

Figure 7: Laser Output Power (Left) and Laser Output Spectrum (Right) Measurements

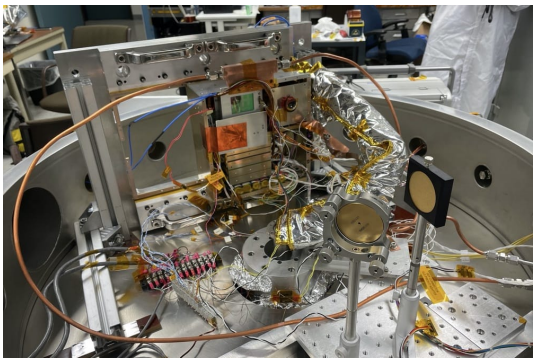

Figure 8: Payload End-to-end Test 4 Setup

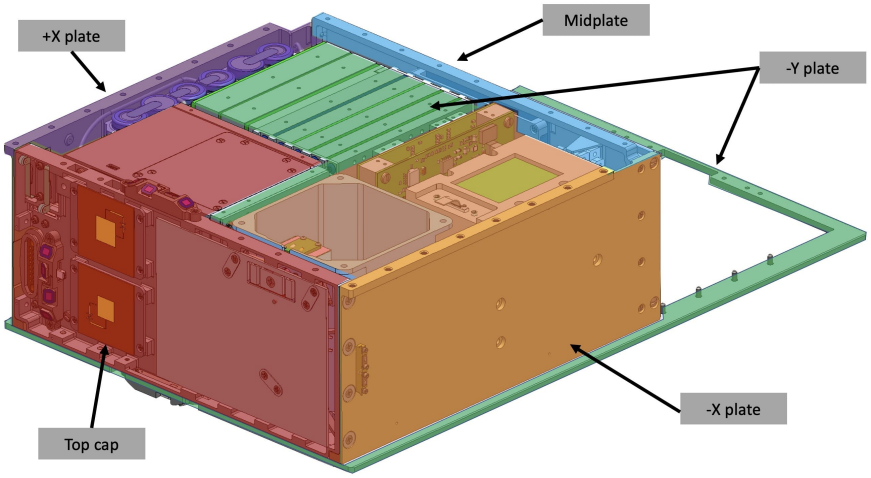

Figure 9: Upper Spacecraft Assembly with the Five Primary Sub-Assemblies Highlighted

Upper Spacecraft I&T

The upper spacecraft consists of the C&DH, avionics battery, payload, and most of the ADCS and radio components. The only other components on the spacecraft are the propulsion system, solar panels, and some radio and ADCS components which mount to the propulsion system. The upper spacecraft is made up of five mechanical subassemblies: the $-$Y plate, the +X plate, the $-$Z plate (aka "top cap"), the $-$X plate, and the "midplate". Figure 9 shows the locations of each sub-assembly. Each sub-assembly was built separately, then the four "walls" were assembled onto the $-$Y plate. Positioning pins were designed such that the cornerstone of the spacecraft would always be established in the +X / $-$Y / $-Z$ (top cap) corner. After this reference was established, the rest of the subassemblies could be torqued down securely. Figure 10 through Figure 12 shows how these subassemblies came together for the final installation.

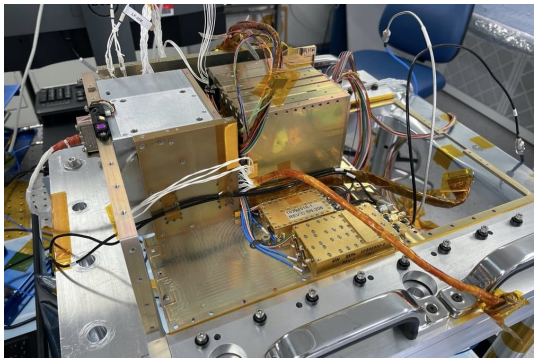

Figure 10: Partially Integrated Upper Spacecraft

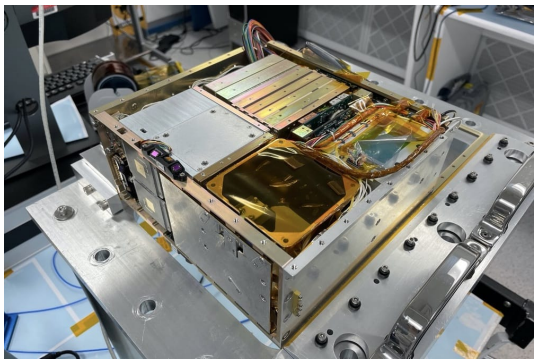

Figure 11: Integrated Upper Spacecraft Prior to +Y Plate Installation

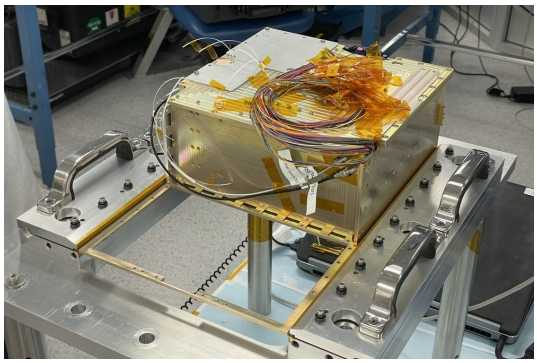

Figure 12: Integrated Upper spacecraft with the +Y Plate Installed for Transport to GT

Propulsion System I&T

The Lunar Flashlight Propulsion System was designed and assembled at Georgia Tech,[9] and was the first item to be integrated into the spacecraft following the arrival of the upper spacecraft to GTRI's

C-SHAFT facility. Integration was followed by functional and thermal performance testing of the LFPS, as well as a thruster replacement.

Propulsion System Integration

The LFPS integration process began with initial electrical compatibility tests prior to shimming and mating with the upper spacecraft. After performing a standalone functional test of the propulsion system along with a safe-to-mate procedure, the LFPS was electrically mated to the spacecraft for an end-to-end electrical test (Figure 13). Once communication was established, the spacecraft C&DH system could successfully command the LFPS and receive telemetry using the XACT as a relay.

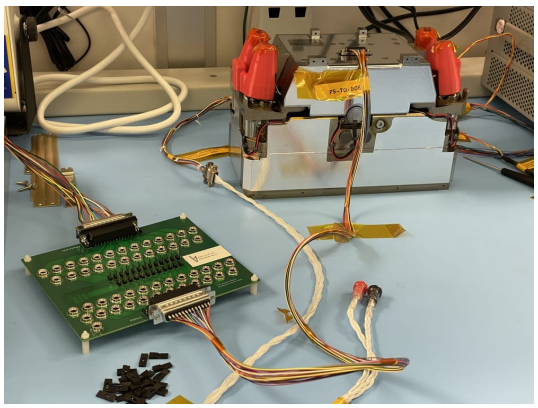

Figure 13: Initial End-to-End Electrical Test of Prop System with Spacecraft

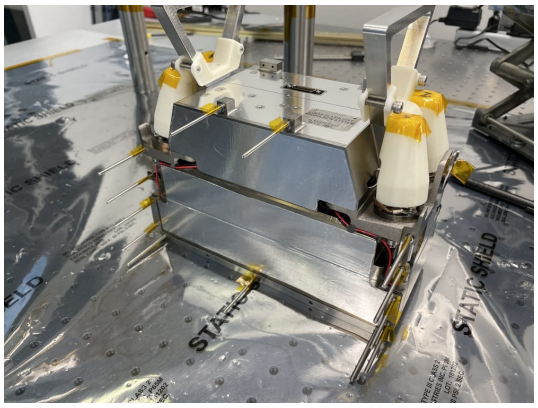

Figure 14: Handles Installed on the LFPS with Shims Loaded and Ready for Integration

Installation of the LFPS into the spacecraft required the selection and installation of shims. Different shims were tested until an optimal fit was found. Threaded rods were used to hold the shims and align the propulsion system with the upper spacecraft while it was lowered onto the upper spacecraft chassis (Figure 14). After fully lowering the LFPS onto the chassis (Figure 15), the rods were replaced with screws. Additional shims were added at the other interfaces between the LFPS and the upper spacecraft, then screws were installed at those interfaces.

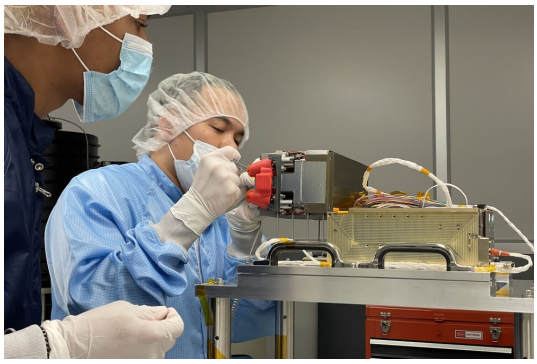

Figure 15: Lowering the Propulsion System Onto the Spacecraft Using Threaded Rods

Following propulsion system integration, the +Z components were installed. This included two Iris radio antennas, a sun sensor, and an RBF power inhibit assembly.

The non-flight handles used for maneuvering the LFPS became the primary spacecraft handling feature following integration. These were used to help move the spacecraft inside of the NEA Scout-provided Dreadnaught fixture and between various other fixtures.

Thruster Replacement

After the propulsion system had been integrated into the spacecraft and the spacecraft had undergone random vibration testing, additional random vibration and hot fire qualification testing was performed on spare thrusters. This testing showed that a feed tube configuration used by one of the flight thrusters was likely to develop a leak during flight, necessitating the replacement of that thruster.

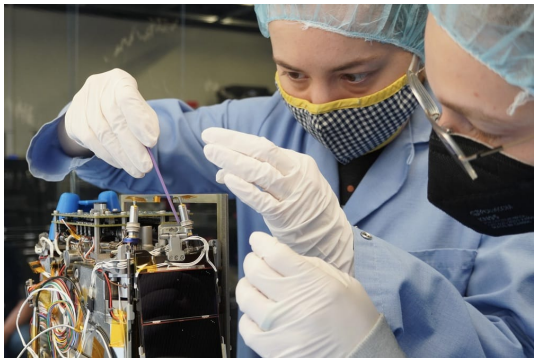

Figure 16: Removal of Thruster

Replacement of the thruster was a collaborative effort between MSFC, the thruster vendor, GT, and JPL. All peripheral hardware attached to the "muffin tin" (which covers the LFPS electronics) was carefully removed. This included the +Z Iris radio antennas, +Z sun sensor, BCT solar panels, and RBF pin assembly. Then the −Y backplate was gently pulled back to allow the muffin tin to be extracted, allowing access to the thruster and its electrical connections. Staking had been used on the thruster heater and thermocouple connectors and this had to be carefully removed. After this, the thruster fasteners were removed and the thruster was taken off the LFPS (Figure 16).

The new thruster was installed and a flow test was performed with helium to ensure expected flow through the thruster (Figure 17). The system was then reassembled, first with installation of the "muffin tin", followed by installation of peripheral hardware and solar panels (Figure 18). Staking was applied to fastener heads as an additional locking measure since workmanship would not be tested with an additional random vibration test. Finally, the fully reassembled spacecraft was placed in a vacuum chamber where a full thruster preheat cycle was successfully performed.

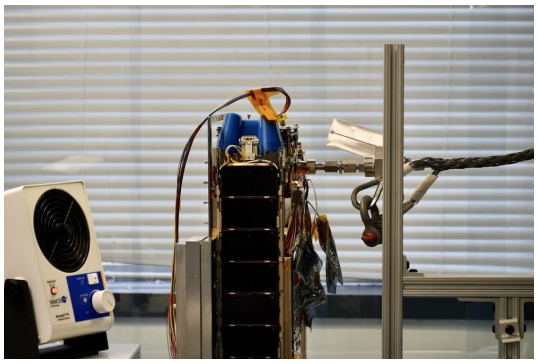

Figure 17: Flow Test with New Thruster

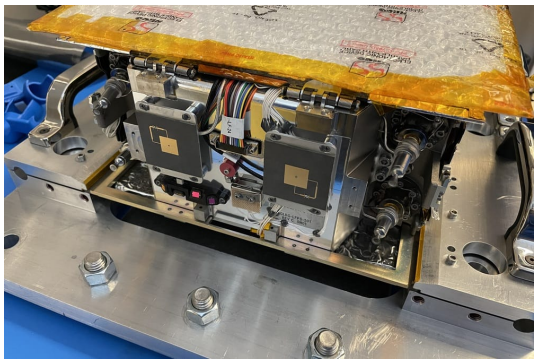

Figure 18: Re-Installed Peripherals at Start of Thruster Preheat Test

Propulsion System Tests

The propulsion system underwent a variety of functional testing following integration. First, a standardized functional test was developed as part of the larger spacecraft full functional test procedure. This test verified two-way communication between the C&DH system and LFPS through the XACT, verified temperature and pressure sensor feedback, exercised all heater channels at safe temperatures, and optionally exercised the valves.

Second, a thruster preheat test was developed to test the performance of the heaters in the integrated system. The LFPS thrusters must preheat to $> 380\,^{\circ}\mathrm{C}$ before they can begin maneuvers. This preheat operation is one of the most power-intensive operations performed by the spacecraft and the warm-up curve depends on the voltage drop of the integrated system, which was unknown prior to integration. Identifying this curve was critical for understanding the operational power budget and for planning sequences.

The test was performed while the spacecraft was under vacuum, at both a hot and a cold plateau of the TVAC test (Figure 19), as well as after the thruster replacement. This test mirrored thruster preheat testing performed during acceptance testing of the propulsion system, but now occurred using commanding and power provided through the spacecraft. The preheat was successfully completed within the power requirements at both the hot and cold TVAC plateaus. The cold test struggled to reach the desired initial firing temperature, which was due to two non-flight-like conditions. First, the propulsion system will be sun-pointing during preheat, so the system should be much warmer. Second, the GSE-supplied current was only 2.5 A rather than the 4.7 A expected from the solar arrays when preheating during flight. The higher current will translate to a higher input voltage and higher preheat power during flight.

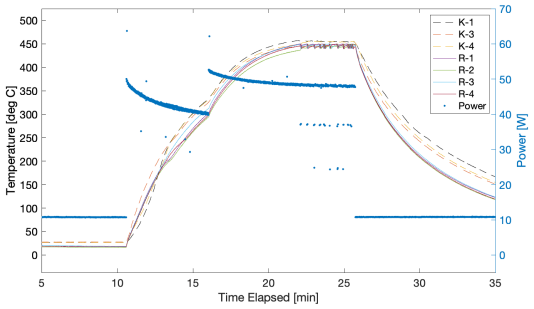

Figure 19: Thruster Preheat Results During TVAC Hot Dwell

Finally, a thruster valve commandability test was performed. This showed that for each valve commanded by the XACT, the appropriate valve on the propulsion system was actuated. First, each thruster nozzle was sealed with Kapton tape. Then, with the propellant tank isolation valve open, each thruster valve was individually actuated via an XACT ManualBurn command. Helium which was left in the propellant tank to ensure a positive pressure now escaped through each nozzle under test, pressing against the tape to create a visual indicator of the active thruster valve. The location of each indicating valve was compared with the XACT ICD, which confirmed the proper valve was actuating.

Solar Array I&T

Following integration of the propulsion system into the spacecraft, the four solar arrays were integrated, then tested for functionality. This was performed after LFPS integration since three of the solar arrays utilized mounting points on the propulsion system.

Solar Array Integration

The two BCT arrays were installed on the +Y and −Y faces of the spacecraft. Non-flight screws were installed opposite the spring-loaded brackets to keep each BCT panel stowed against the side of the spacecraft while it was outside of the dispenser.

The two MMA tri-fold arrays were installed on the +X and -X spacecraft faces. This process included the installation of a spring-loaded burnwire-triggered launch cage for stowing the panels, as well as the application of Kapton-covered padding for protecting the stowed panels.

As part of the solar array installation process, the pigtail harnesses on all four arrays were cut to size and soldered into Cristek Micro Strip connectors (Figure 20).

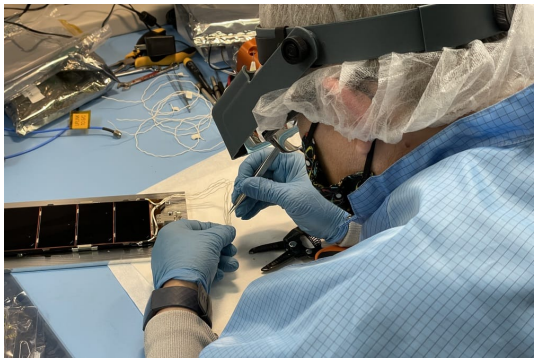

Figure 20: Solar Array Harnessing

To protect the BCT solar arrays during dispenser installation, launch, and deployment, snubbers and bumpers were installed. Snubbers are silicone pads mounted to the spacecraft chassis that sit under the stowed arrays. They dampen vibration and prevent contact between the panels and the spacecraft chassis.[12] Arrays of snubbers were installed on the +Y and -Y faces of the spacecraft using Momentive RTV566 silicone sealant (Figure 21).

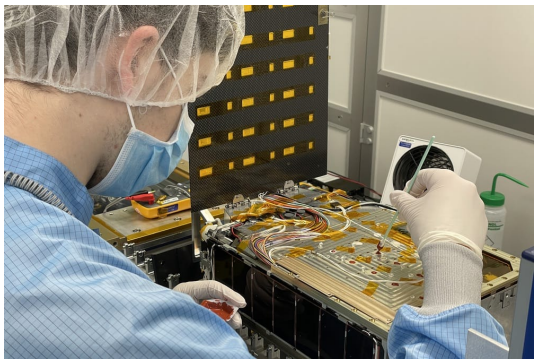

Figure 21: Installation of Solar Array Snubbers

Bumpers are 3D-printed ULTEM spacers that keep the solar arrays from contacting the dispenser (Figure 22). Optimal locations for the bumpers were determined by sliding the spacecraft into and out of the dispenser-emulating segment of the Dreadnaught fixture. They were adhesed to the sides of the BCT arrays using Henkel 9394.

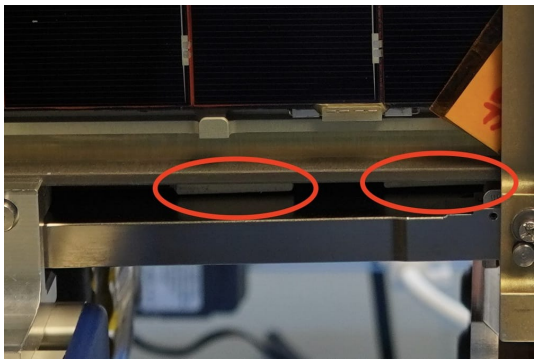

Figure 22: Bumpers Keep the Solar Cells from Touching the Dispenser Door

Solar Array Tests

The Gravity Offload Fixture (GOLF) provided by the NEA Scout project was used to perform solar array deployment tests (Figure 23). This fixture uses constant force springs to counteract gravity, allowing the solar array springs to deploy the panels vertically in a simulated zero-g setup. For the MMA tri-fold panels, burnwires were commanded on briefly by an

operator, and each mechanism successfully demonstrated an appropriate melting of the melt rod and subsequent deployment. For the BCT panels, the GOLF included two motor-actuated brackets which held the panels in a stowed position. Upon manual activation of the motors, the brackets retracted, simulating deployment from the flight dispenser. This test also demonstrated a successful deployment.

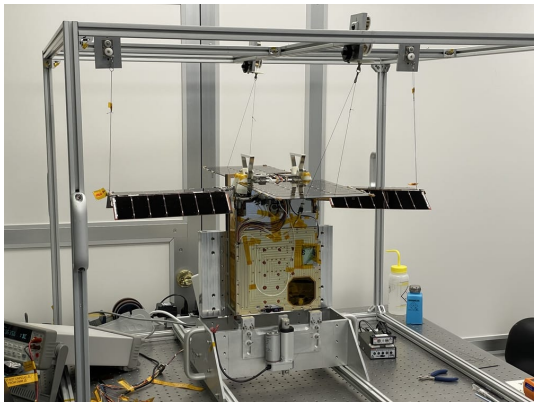

Figure 23: Solar Array Deployment Test Performed with Gravity Offload Fixture

Following the final integration of solar arrays, a charging test was performed with a 500 W lamp to ensure that the spacecraft EPS could receive power from each array (Figure 24). The EPS disables charging from certain solar array channels depending on the avionics battery voltage, so the battery had to be drained below these thresholds to test charging with each array. This test was successful, capturing approximately 100mA from each MMA array and 250mA from each BCT array.

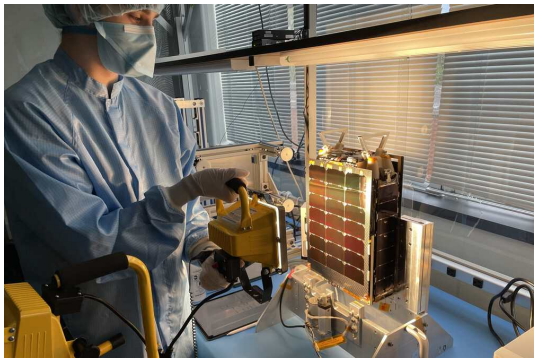

Figure 24: Illuminating the +Y BCT Panel

Environmental Testing: Random Vibration

A random vibration test was performed to show that the spacecraft, as designed and built, can survive the vibration loads expected during launch. The test profile for each axis was determined by a JPL dynamicist working with values given by the launch provider. For Lunar Flashlight, test profiles were first established assuming the Space Launch System (SLS) would be the launch vehicle. The project switched to a SpaceX Falcon 9 launch vehicle, but as the new vibration profiles were enveloped by the previous SLS profiles, no changes needed to be made, and the test was considered valid for either launch vehicle.

The Random Vibration test was performed at GTRI's Cobb County Research Facility (CCRF), following the test plan in Table 2. The fixture used for holding the spacecraft during Random Vibration was shared by the NEA Scout project due to the similarities between the two spacecraft (Figure 25).

Table 1: Random Vibration Test Plan

Test	Description
1	Hardware Functional Test
2	X-axis Resonance Search
3	X-axis Random Vibration Test Profile
4	Rotate Spacecraft
5	Z-axis Resonance Search
6	Z-axis Random Vibration Test Profile
7	Reconfigure Shaker for Vertical Test
8	Y-axis Resonance Search
9	Y-axis Random Vibration Test Profile
10	Hardware Functional Test

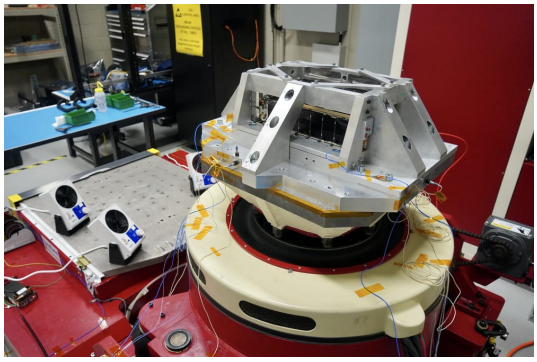

Figure 25: Random Vibration Z-Axis Setup

Before and after the random vibration environmental test, laser alignment tests were performed to record reference measurements of the laser taken using the onboard optical detector. To perform this test, the laser was set up to face an off-axis parabolic mirror. This mirror was then adjusted to face a gold-coated diffuse reflectance target. Finally, short laser firing sequences were run, and neutral-density filters were added to attenuate the detector signal until it measured non-saturated values.

After completing the random vibration environmental test, another laser alignment test was done to compare system performance. This setup mirrored the pre-vibration setup including the final neutral-density filter configuration. As part of this test, the laser output was also captured with a FLIR SC6100 thermal camera (Figure 26).

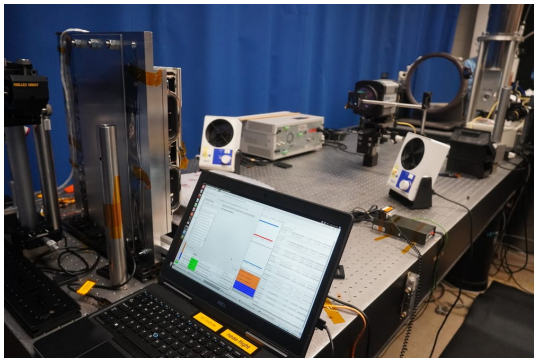

Figure 26: Laser Thermal Image Capture

Environmental Testing: EMI/EMC

An Electromagnetic Interference / Electromagnetic Compatibility (EMI/EMC) test was performed in an anechoic chamber at GTRI's CCRF location (Figure 27). Lunar Flashlight has two pairs of planar patch antennas, one on the propulsion system (+Z) side and one on the payload radiator (−Z) side. This test was designed to confirm the capability of the spacecraft to communicate using each pair of antennas. For each antenna pair, a "plugs-in" test was performed, where operators adjusted the spacecraft and GSE settings to achieve a reliable RF lock on uplink and downlink channels. This was followed by a "plugs-out" test, where operators disconnected the spacecraft from external power and wired communications, and used the settings determined previously to communicate with the spacecraft.

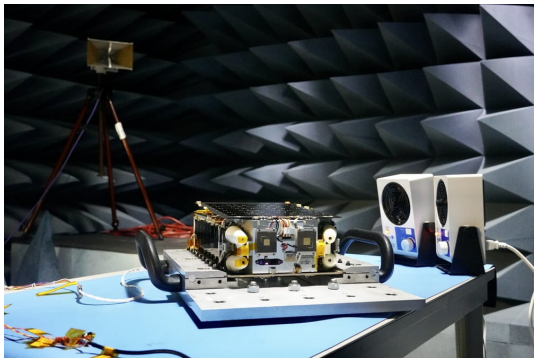

Figure 27: EMI/EMC Test Setup

By following the test plan in Table 2, this test successfully showed that while fully disconnected from GSE, the spacecraft could communicate wirelessly in full-duplex using each pair of antennas.

Table 2: EMI/EMC Test Plan

Test	Description
1	"Plugs-In" +Z antenna test to verify setup.
2	"Plugs-Out" +Z antenna test, with checkout of payload and propulsion system. (No external power or wired UART)
3	Rotate spacecraft 180° for -Z test.
4	"Plugs-In" -Z antenna test to verify setup.
5	"Plugs-Out" -Z antenna test, with checkout of payload and propulsion system. (No external power or wired UART)

ADCS Testing

After final integration of the XACT and its external sun sensors, tests were performed to ensure each XACT component was integrated and operating correctly.

The XACT utilizes sun sensors to keep the spacecraft's solar arrays sun-pointing by default, ensuring the spacecraft stays powered with batteries charged. The functionality of these sensors was tested after installation to ensure proper connection, orientation, and operation (Figure 28). This test utilized a 500 W work lamp as a basic solar simulator.

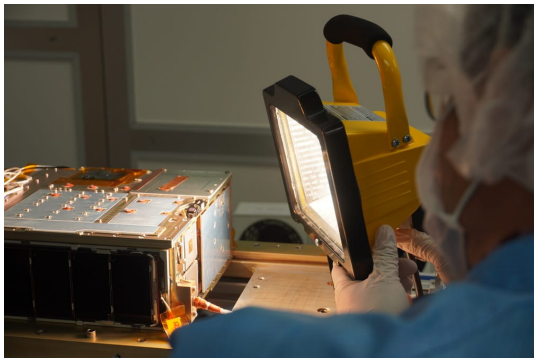

Figure 28: Test of the +Y XACT Sun Sensor

On Lunar Flashlight, each sun sensor assembly includes four photodiodes each with unique pointing vectors. For each assembly, the following test was performed. First, the lamp was positioned directly parallel with the boresight of the assembly. Then the sun vector telemetry was checked to confirm the XACT was detecting the sun along the axis of the tested sensor. Next, the light was moved approximately 30° from the boresight and the telemetry was examined to confirm the XACT's sun vector had moved appropriately. Finally, the light was moved

approximately 30° from the boresight in the opposite direction, and the telemetry was again checked to confirm the updated sun vector matched expectations. This test was performed on all four sun sensor assemblies.

The XACT includes a star tracker or stellar reference unit (SRU) which is used to determine the spacecraft's attitude during flight. It uses a camera to measure the brightness of stars in the field of view. These measurements are then compared to an internal star field catalog using a pattern-matching star identification algorithm.[13]

Following integration of the XACT into the spacecraft, the SRU was tested using a JPL-developed star field simulator (SFS).[14] This simulator works by generating a star field image onto a display placed in front of the XACT's star tracker camera (Figure 29). First, a functional test was performed to calibrate the SFS, ensuring that the XACT was able to detect the simulated stars and determine where it was pointing in the simulated environment. After confirming the setup and basic functionality of the SRU, phasing tests were performed for each axis.

For each phasing test, the SFS was configured to display a star field, then rotate the field around a specific axis at 0.5 °/s for approximately 180 seconds. As the star field rotated, the XACT's SRU-based attitude vector was reviewed to confirm that it was rotating along the expected axis and in the appropriate direction.

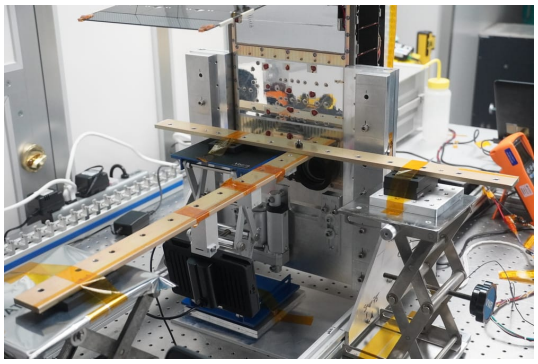

Figure 29: Test of the XACT Star Tracker Using Starfield Simulator Display

While the XACT camera is primarily for use as a star tracker, it can be used to capture images during operations. This functionality was tested using a few team members as subjects (Figure 30).

Figure 30: Test Image Captured with the XACT Onboard Camera

Thermal Patch Installation

Thermal analysis was performed on the final spacecraft design, which resulted in recommendations for the installation of thermal control surfaces. Silver coated Teflon was installed on five faces of the spacecraft, including the payload's optical receiver cryogenic radiator, to increase the passive cooling capability of the system (Figure 31). After installing the material, Scotch-Weld 2216 staking was added to provide additional bonding. Finally, Eccobond 57C was applied to ground each Teflon sheet to the spacecraft chassis, and each Eccobond stripe was covered with an overcoat of Arathane 5750.

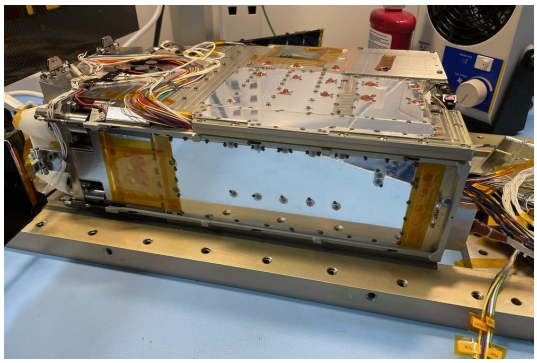

Figure 31: Silver Teflon Applied to Spacecraft

Mass and CG Measurements

A measurement jig was developed by GTRI to aid in the determination of the spacecraft's center of gravity (Figure 32). This fixture was made using 80/20 t-slot rails combined with 3D-printed rails, and could be reconfigured to hold the spacecraft on each axis. In each configuration, the spacecraft sat on two balance points, with the ability to rock along

the axis created by those points. Careful adjustments were made until the spacecraft was balanced on the two points. Once fully balanced, the position of the balance points was measured with respect to the spacecraft, as they indicated the center of gravity of the spacecraft along a specific axis. This test was repeated for all three axes to calculate the three-dimensional center of gravity. After this, a mass measurement was performed, confirming the unfueled spacecraft met the project's mass requirements at 11.5 kg.

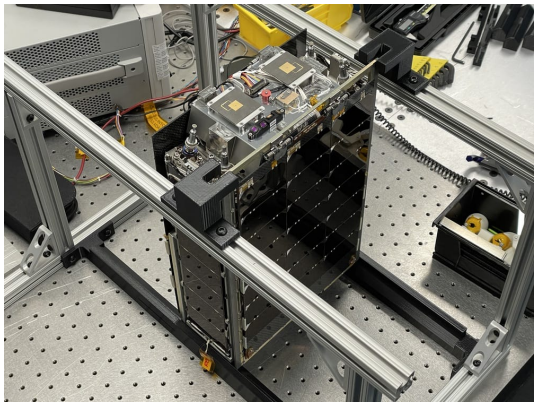

Figure 32: Measuring the Y-axis Center of Gravity

To aid in transferring the spacecraft from its carrying fixture to the CG fixture, a sheet metal handle was manufactured (Figure 33). Once placed into service, this handle continued to be used as an aid along with the propulsion system handles for two-person transfers of the spacecraft between MSFC and JPL fixtures.

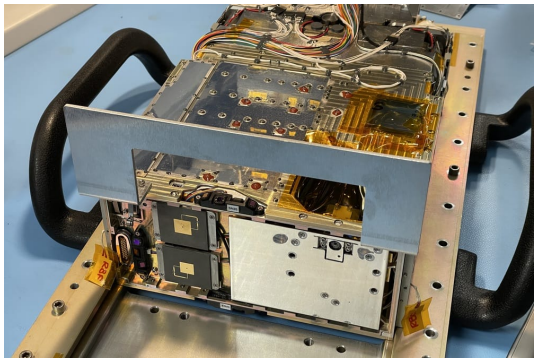

Figure 33: Aluminum Handle Used for Carrying Spacecraft Between Fixtures

Environmental Testing: TVAC

Spacecraft-level thermal vacuum (TVAC) testing was performed to demonstrate the functionality of the spacecraft in the space environment. A 120-hour bakeout was also combined into the hot dwell portions of the test. The TVAC test required a vacuum of $< 1\times10^{-5}$ torr and two thermal cycles with hot plateaus at 40 °C and cold plateaus at −10 °C. The test outline is shown in Figure 34.

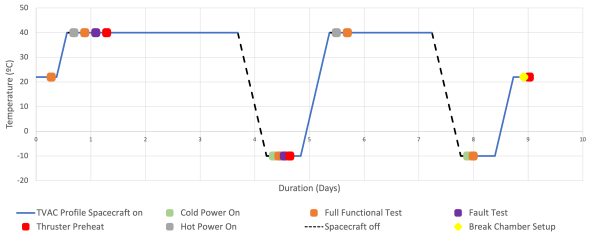

Figure 34: LF TVAC/Bakeout Test Plan

A LACO 1P23232 single-walled thermal vacuum chamber was utilized for this test. Initial tests with the chamber's single JULABO chiller and a mass model showed that a more powerful system would be needed to heat and chill the spacecraft to the necessary temperatures. This was accomplished by augmenting the system with a copper shroud and an additional JULABO chiller (Figure 35). The shroud was constructed out of 1/8" 110 copper sheets and surrounded by seven loops of 1/2" OD 122 copper tubing. The second chiller pumped Thermal C5 fluid through this tubing to heat or cool the shroud.

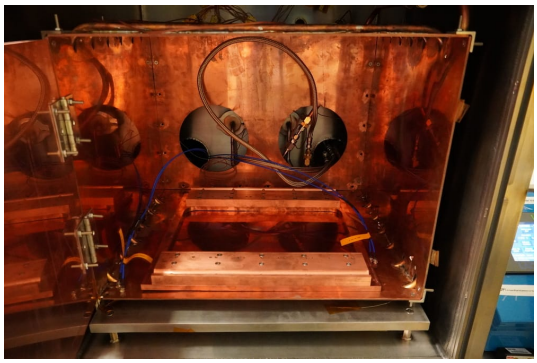

Figure 35: Copper Handling Fixture and Liquid-Cooled Copper Shroud

Five aluminum rods wrapped in copper gauze were placed between the tubes on the copper box and the "platen" of the LACO chamber to thermally connect it to the primary chiller. With both chillers set to −40 °C, this new setup achieved mass model temperatures below the −10 °C requirement.

For the flight system test, the standard aluminum spacecraft handling fixture was replaced with a copper fixture to provide higher thermal conductivity between the chillers and the spacecraft. Copper gauze was also added between the spacecraft chassis and the shroud to provide additional thermal pathways (Figure 36).

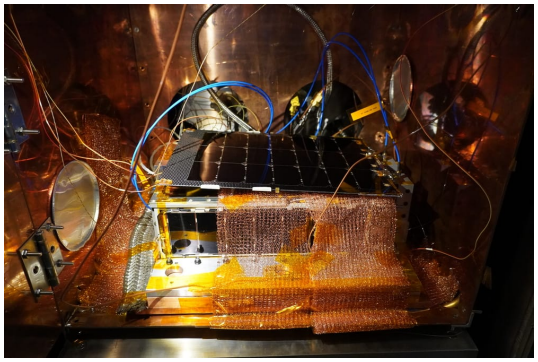

Figure 36: Spacecraft in TVAC Chamber

Thermocouples were applied to strategic locations on the CubeSat for this test (Figure 37). Data from these thermocouples augmented the spacecraft thermal telemetry, allowing operators to effectively monitor and set the temperature of the system even when the spacecraft was powered off. Additionally, this data was logged to allow for future improvements to the spacecraft's thermal model.

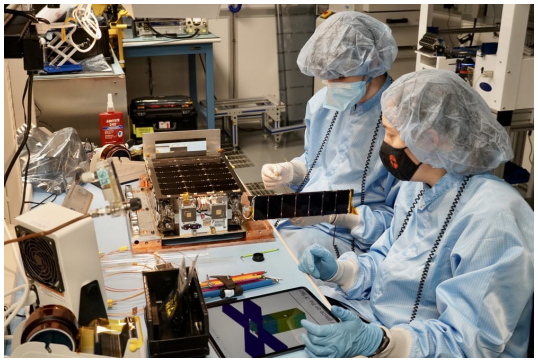

Figure 37: Installing Thermocouples for TVAC

The thermal vacuum test was completed over 10 days with 24-hour in-person monitoring. A team of three to four core members was responsible for running functional and other prescribed tests, while approximately 10 others were responsible for the 24-hour monitoring in shifts. Two hot and cold cycles were performed, with the hot plateaus being extended to cover the bakeout requirement. Witness plates were also used to analyze contamination released from the system during bakeout. The last part of each thermal cycle included a non-operational portion, where the spacecraft was powered off to assist in the temperature ramp from hot to cold. This TVAC test was successful, satisfying the temperature cycling requirements and confirming that the spacecraft can operate effectively across its expected temperature range.

Helium Purge Test

A helium purge test was also performed as part of the vacuum chamber environmental testing campaign. As part of the launch process, the Falcon 9 stage housing Lunar Flashlight will be purged with helium. Certain electrical devices, particularly microelectronic mechanical systems (MEMS), can be damaged by helium exposure, so the launch provider required a helium purge test. This test consisted of placing the spacecraft in a helium environment at a pressure of approximately 15 psi for 24 hours. To simulate flight, a vacuum was then pulled, followed by spacecraft power-on and a functional test to verify continued nominal operation.

To purge the chamber with helium, a helium K-bottle was connected to a single stage regulator which regulated the bottle pressure of 2000-3000 psig down to approximately 1 psig. The output of the regulator was then connected to a flow meter which fed into the chamber. The flow meter allowed operators to monitor the flow rate into the chamber and measure the leak rate of the system. To minimize the leak rate, multiple c-clamps were placed around the door to further compress it against the o-ring seal.

To start the test, a rough vacuum of < 1 torr was achieved. Then, helium was pumped in at approximately 1 psig through the regulator and flow meter. As the chamber reached equilibrium, the flow rate decreased to the leak rate. This setup was held for 24 hours, and then the chamber was again pumped down to vacuum. This was followed by the full functional test which verified that the spacecraft continued to function nominally.

Operational Testing

Two tests were performed as a collaboration between the Operations and SI&T teams with a portion of both carried out on the fully integrated spacecraft at GT. These tests served as an opportunity for the Operations team to gain experience working directly with the spacecraft, acquiring higher fidelity data than the testbed could provide, while also gathering data needed to verify requirements were met.

The Day in the Life test exercised various mission scenarios, from the initial safe mode sequence at post-deployment power-on, to autonomous propulsion maneuver command sequences. The Fault Protection test explored flight software's responses to various fault scenarios, ensuring that the system responded to faults as documented and successfully enforced autonomous flight rules.[15]

Dispenser Fit-Check

A dispenser fit-check was performed with support from the launch integrator. Using the Dreadnaught fixture, the spacecraft was inserted into the spring-loaded dispenser (Figure 38). The team demonstrated that the dispenser door could properly latch closed, and that the spacecraft avionics battery could be charged through the maintenance port while the spacecraft was stowed.

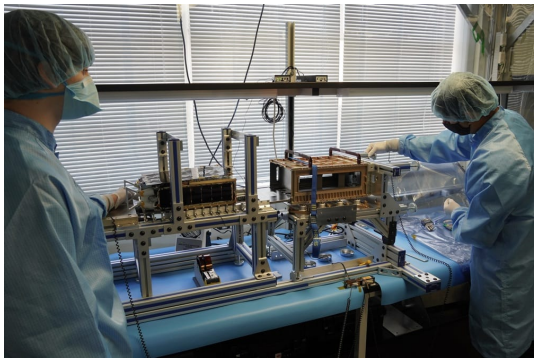

Figure 38: Installation of Spacecraft into Dispenser Using Dreadnaught Fixture

Final SI&T Activities

A collection of closeout activities was performed to wrap up the SI&T campaign. This included installation of the flight avionics battery, cleaning of solar arrays, additional staking of external wires, and the installation and testing of new flight software releases. Once these final SI&T activities were completed, the spacecraft was nitrogen-purged and placed in storage awaiting fueling.

LESSONS LEARNED

Numerous lessons were learned during this mission's SI&T process, from the value of harness engineering support, to the benefits of a flight-like testbed and appropriate tools for accessing and manipulating data.

Harness Engineering

Effective harness engineering is extremely valuable when working on a project of this complexity and compactness. The lack of a harnessing engineer led to significant wiring issues during integration. For example, the team frequently spent lots of time determining how to fit harnesses into allocated spaces. Unwieldy laser power cables had to be replaced with thinner and more precisely manufactured busbars. Shielding and strain relief tape were often reworked multiple times until they met bend radius requirements. Interference with staking on an avionics battery harness required removal of material from the spacecraft chassis.

SpaceWire data corruption was another issue that could have been avoided with more in-depth harness engineering. It was discovered that PWM-controlled heater wires running near a SpaceWire harness caused intermittent data integrity issues when active. This was resolved with a flight rule limiting when the heaters are used, but could have been avoided with better routing or shielding.

Imprecise lengths of cables also caused trouble during SI&T. For example, unexpected differences in the length of coax patch antenna cables necessitated an unplanned flip of antenna positions, which caused confusion during later RF testing when equipment was set up near the wrong antennas. Also, excess length in the propulsion system power and data harness had to be handled on the external surface of the spacecraft, which necessitated a complicated routing and staking strategy.

Limited harness modeling also made it difficult to estimate the voltage drop and related power limitations that each subsystem would experience, prior to integration. This was especially concerning for the propulsion system, which was one of the last subsystems to be integrated, yet had high power requirements for preheating the thruster catalyst beds.

Dimensional Checks

The value of dimensional checks and "fit checks" was underscored throughout the SI&T process. The team used the rapid prototype approach for various fit checks, successfully testing out new designs using 3D-printed models. For example, prior to manufacturing metal busbars, full-size 3D-printed models were created. These were used to quickly iterate the design prior to starting the more complicated metal fabrication process. When plans were being developed to modify the payload radiator, a 3D-printed model was created to test the fit of the new design. This approach was critical, as an improper modification to the radiator could have necessitated the manufacturing of an entirely new part, with significant delays.

Mishap Prevention and Detection

A few mishaps during the SI&T process emphasized how appropriate documentation, procedures, and hardware protections can prevent accidents or

reduce their effects. One mishap was the accidental application of 14 V to a 5 V C&DH power rail. In this case, internal protection diodes clamped the voltage and no hardware needed to be replaced, but the follow-up testing and analysis caused delays in the schedule. A better-designed GSE setup could have avoided this. For example, an external interface board could have monitored for overvoltage before passing power on to the spacecraft. The spacecraft power-on procedure was modified after this event to add additional checks and precautions prior to applying power.

Another mishap occurred on the testbed, where a C&DH board received 12 V on a 3.3 V line. The root cause of this issue was traced back to differences between the flight and testbed units and a lack of documentation about these differences. Better access to schematics as well as documentation or training about these differences could have kept this scenario from occurring.

During payload integration, a concealed wire on the APLE subassembly broke off, causing the detector current telemetry to jump to the maximum value. In ambient conditions, outside of payload tests where the detector was in a low-light condition and properly cooled, the associated telemetry channel was generally saturated. As such, it was considered N/A (i.e. no pass/fail criteria) in the recurring system functional checkout tests. This assumption led to the damage being undiscovered until after the upper spacecraft had been completely integrated and transported to GT, at which point the repair caused a significant schedule impact. Future tests ensured this value was checked, but this scenario demonstrated the risk of failing to provide pass/fail criteria for telemetry channels.

Flight-Like Testbed

The testbed is a crucial part of any space mission, and ideally it can replicate all functionalities, modes, and operations of the spacecraft. For the Lunar Flashlight testbed, a few deviations in capabilities made it difficult to rehearse for operations or troubleshoot the spacecraft, leading in some cases to large schedule impacts.

Differences between the testbed and flight C&DH units meant that separate software and firmware releases had to be compiled for each unit. One hardware difference between the two units was the number of outputs available for driving heater enable lines, with the flight unit capable of enabling more outputs than the testbed unit. Additional logic for these channels could not be tested on the testbed, so a bug in this firmware was not discovered until after installation on the spacecraft. Additionally, this difference made it impossible to test many command sequences on the testbed prior to installation on the spacecraft, in cases where commands were included which referenced nonexistent output lines.

The spacecraft avionics stack includes an interface board which connects to many subsystems and provides heater switching and other capabilities. A similar board did not exist in the testbed during SI&T. This helped to conceal an RS-422 pinout issue on the flight interface board which was not discovered until integration of the propulsion system. It also limited the ability to test power draw and flight software functionality prior to full spacecraft integration.

Finally, the Iris radio was represented in the testbed only through an FPGA development board interface simulator. While this allowed for testing of the command and telemetry interface, it did not recreate the actual power characteristics or behavior of the radio. For example, the Iris requires a specific power-up signal sequence, while the simulator does not. As a result, flight software did not account for this sequence, which led to a power-up anomaly being identified late in the SI&T process. This necessitated a flight software update, which carried a significant schedule impact.

These gaps in testbed fidelity meant that many development tests could not be performed on the testbed prior to running on the flight system. This placed a higher risk on the flight hardware throughout the SI&T process. While it may not be feasible to implement all functionality in a system testbed, these experiences showed that a project can avoid many issues by sharing as much functionality between the testbed and flight hardware as possible.

Data Accessibility

During subsystem and spacecraft testing, the accessibility of data played a large role in resolving issues. AMPCS,[16] the JPL-developed data processing and control system in use by this project, is capable of providing telemetry and uplinked commands in a CSV format. A post-processing script was developed to compile this data into Excel spreadsheets and HTML Plotly-based interactive charts. These spreadsheets and interactive graphs could easily be shared without requiring any special software to use, making it easier to discuss and solve problems related to each subsystem. This post-processing software was also extended to process science data from Lunar Flashlight's science payload. This data con-

sists of optical detector feedback as well as temperatures, voltages, and current telemetry from the optical system. Being able to quickly interact with this data made the setup process much easier during tests of the laser.

Cross-institution IT policies meant that many of the SI&T computers were not network-connected once delivered to Georgia Tech. This presented data accessibility issues as well as hurdles to keeping configurations synchronized between computers, as information was previously funneled through a centralized GitHub instance. These issues were somewhat rectified through the use of a bare Git repository on a machine with access to the GitHub server, which could act as an intermediary between networks. However, a better private network setup would have saved time.

These experiences showed that data accessibility was key to making the SI&T process run smoothly. The more steps it took to process data and deliver it to relevant parties, the harder it was to iterate and solve problems. Development of data processing scripts helped to ease this pain and get problems solved more quickly.

CONCLUSION

Following fueling of the propulsion system at MSFC in fall 2022, Lunar Flashlight is expected to launch in late 2022 or early 2023. After launch it will perform a lunar orbit insertion and enter its science phase, searching for water ice in the craters of the Moon's south pole. The Systems Integration and Test campaign for this project was an intense collaborative effort between many organizations, including the Jet Propulsion Lab and Georgia Tech. This experience resulted in many lessons learned by all participants which will inform future missions.

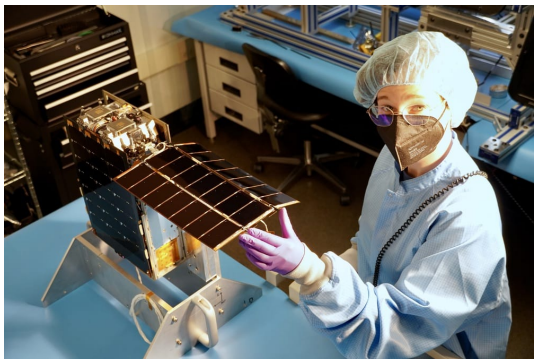

Figure 39: Spacecraft Prior to Fueling

ACKNOWLEDGEMENTS

A portion of this research was carried out at the Jet Propulsion Laboratory, California Institute of Technology, under NASA contract 80NM0018D0004. Research was also performed under California Institute of Technology subcontract 1665462. Additionally, the Lunar Flashlight integration and test campaign would not have been completed without the help of many individuals.

At the NASA Jet Propulsion Laboratory and affiliated organizations, the following individuals supported this work: Vinh Bach, Mahmood Bagheri, Frank Barone, Brandon Burgett, Matthew Chase, Alex Choi, Jesus "Jesse" Cortez, Guillaume Crooks, Oscar Deng, David Foor, Yutao He, Todd Hurst, Sam Islas, Glenn Jeffery, Jerri Ji, Lawrence Johnson, Warren Kaye, Roger Klemm, Matthew Kowalkowski, Kevin Lo, Jessica Loveland, Corentin Lubeigt, Huong Ly, Lauren McNally, Lini Mestar, Arnaud Meyer, Robert Miller, Albert "Ron" Morgan, Sam Mouradian, Duy Nguyen, Kevin Ortega, Christopher Paine, Alex Perez, Frank Picha, Jacqueline "Jackie" Rapinchuk, Aadil Rizvi, Calina Seybold, Anthony Shao-Berkery, Robert Sharka, Chris Smith, Charles Sommer, David Sternberg, Quentin Vinckier, and Karl Yeh.

At the Georgia Tech Research Institute, Eric Brown, Melissa (Missy) Catlin, Hunter Chan, Robert Dunning, David Duperre, Jordan Florence, Ian Harrison, Stephen Hurst, Dylan Jean-Baptiste, Zhitao Kang, Ryan Lewis, Brandon Lovelacez Mason Placanica, Elena Plis, Paul Simmons, Travis Turner, Valentin Richter, Benjamin Quick, Brandon Vaughan, and Yuelan Zhang supported Lunar Flashlight's SI&T campaign.

At the Georgia Institute of Technology's School of Aerospace Engineering, the project was made possible through the work of Michael Hauge, Lacey Littleton, Dillan McDonald, Jishnu Medisetti, Mach Michaels, and Mason Starr.

At the NASA Marshall Space Flight Center and related organizations, Daniel Cavender, Carlos Diaz, Todd Freestone, and Tomas Hasanof supported integration and testing of the propulsion system and provided advice from the NEA Scout project.

REFERENCES

[1] G. M. Huggins, A. Talaksi, D. Andrews, E. G. Lightsey, D. Cavender, D. McQueen, H. Williams, C. Diaz, J. Baker, and M. Kowalkowski, "Development of a CubeSat-

Scale Green Monopropellant Propulsion System for NASA's Lunar Flashlight Mission," in *AIAA SciTech 2021 Forum*, 2021.

[2] B. A. Cohen, P. O. Hayne, B. Greenhagen, D. A. Paige, C. Seybold, and J. Baker, "Lunar Flashlight: Illuminating the Lunar South Pole," *IEEE Aerospace and Electronic Systems Magazine*, vol. 35, no. 3, pp. 46–52, 2020.

[3] B. A. Cohen, P. O. Hayne, C. G. Paine, D. A. Paige, and B. T. Greenhagen, "Lunar Flashlight: Mapping Lunar Surface Volatiles Using a CubeSat," in *46th Lunar and Planetary Science Conference*, 2015.

[4] J. Rapinchuk, J. Loveland, A. Barchowsky, J. Zitkus, T. Hurst, P. Adell, M. Smart, K. Chin, and C. Krause, "Lunar Flashlight Power Subsystem Architecture and Implementation," 2020.

[5] A. Rizvi, "Applying F Prime Flight Software Framework for Lunar Flashlight and Near-Earth Asteroid (NEA) Scout CubeSats," 2019.

[6] M. M. Kobayashi, "Iris Deep-Space Transponder for SLS EM-1 CubeSat Missions," in *Proceedings of the Small Satellite Conference*, 2017.

[7] P. C. Lai, D. C. Sternberg, R. J. Haw, E. D. Gustafson, P. C. Adell, and J. D. Baker, "Lunar Flashlight CubeSat GNC system development," *Acta Astronautica*, vol. 173, pp. 425–441, 2020.

[8] D. Andrews, G. Huggins, E. G. Lightsey, N. Cheek, N. Daniel, A. Talaksi, S. Peet, L. Littleton, S. Patel, L. Skidmore, M. Glaser, D. Cavender, H. Williams, D. McQueen, J. Baker, and M. Kowalkowski, "Design of a Green Monopropellant Propulsion System for the Lunar Flashlight CubeSat Mission," in *Proceedings of the Small Satellite Conference*, 2020.

[9] C. Smith, D. Cavender, L. Littleton, and E. G. Lightsey, "Assembly Integration and Test of the Lunar Flashlight Propulsion System," in *AIAA SciTech 2022 Forum*, 2022.

[10] U. Wehmeier, Q. Vinckier, R. G. Sellar, C. G. Paine, P. O. Hayne, M. Bagheri, M. Rais-Zadeh, S. Forouhar, J. Loveland, and J. Shelton, "The Lunar Flashlight CubeSat instrument: a compact SWIR laser reflectometer to quantify and map water ice on the surface of the moon," in *CubeSats and NanoSats for Remote Sensing II* (T. S. Pagano and C. D. Norton, eds.), vol. 10769, pp. 114–130, International Society for Optics and Photonics, SPIE, 2018.

[11] C. Ryan and D. Foor, "Noise Evaluation of Various High-gain, Very-low-noise Current Sense Amplifier Circuits," in *2021 IEEE Aerospace Conference (50100)*, pp. 1–6, 2021.

[12] NEA Scout Project. Private Communication, 2021.

[13] D. Hegel, "Attitude Determination and Control."

[14] N. Filipe, L. Jones-Wilson, S. Mohan, K. Lo, and W. Jones-Wilson, "Miniaturized Star Tracker Stimulator for Closed-Loop Testing of CubeSats," *Journal of Guidance, Control, and Dynamics*, vol. 40, no. 12, pp. 3239–3246, 2017.

[15] D. McDonald. Private Communication, 2022.

[16] W. L. Quach, L. DeForrest, A. T. Klesh, and J. Schoolcraft, "Adapting a Large-Scale Multi-Mission Ground System for Low-Cost CubeSats," in *SpaceOps 2014 Conference*, 2014.